Journal of Radiation Research, Vol. 64, No. 2, 2023, pp. 358–368
https://doi.org/10.1093/jrr/rrac104
Advance Access Publication: 24 January 2023

The linker of nucleoskeleton and cytoskeleton complex is required for X-ray-induced epithelial-mesenchymal transition

Hiromasa Imaizumi[1,2,*], Kazumasa Minami[1], Miki Hieda[3], Naomasa Narihiro[2] and Masahiko Koizumi[1]

[1]Department of Medical Physics and Engineering, Graduate School of Medicine and Health Science, Osaka University, 1-7 Yamadaoka, Suita, Osaka 565-0871, Japan
[2]Department of Radiological Technology, Faculty of Health Science and Technology, Kawasaki University of Medical Welfare, 288 Matsushima, Kurashiki, Okayama 701-0193, Japan
[3]Graduate School of Health Sciences, Ehime Prefectural University of Health Sciences, 543 Takoda, Tobe-cho, Iyo-gun, Ehime 791-2101, Japan
*Corresponding author. Department of Radiological Technology, Faculty of Health Science and Technology, Kawasaki University of Medical Welfare, 288 Matsushima, Kurashiki, Okayama 701-0193, Japan. E-mail: imaizumi@mw.kawasaki-m.ac.jp; Tel: +81-86-462-1111; Fax: +81-86-464-1109
(Received 7 August 2022; revised 13 November 2022; editorial decision 19 December 2022)

ABSTRACT

The linker of nucleoskeleton and cytoskeleton (LINC) complex has been implicated in various functions of the nuclear envelope, including nuclear migration, mechanotransduction and DNA repair. We previously revealed that the LINC complex component Sad1 and UNC84 domain containing 1 (SUN1) is required for sublethal-dose X-ray-enhanced cell migration and invasion. This study focused on epithelial-mesenchymal transition (EMT), which contributes to cell migration. Hence, the present study aimed to examine whether sublethal-dose X-irradiation induces EMT and whether LINC complex component SUN1 is involved in low-dose X-ray-induced EMT. This study showed that low-dose (0.5 Gy or 2 Gy) X-irradiation induced EMT in human breast cancer MDA-MB-231 cells. Additionally, X-irradiation increased the expression of SUN1. Therefore, SUN1 was depleted using siRNA. In SUN1-depleted cells, low-dose X-irradiation did not induce EMT. In addition, although the SUN1 splicing variant SUN1_916-depleted cells (containing 916 amino acids [AA] of SUN1) were induced EMT by low-dose X-irradiation like as non-transfected control cells, SUN1_888-depleted cells (which encodes 888 AA) were not induced EMT by low-dose X-irradiation. Moreover, since the Wnt/β-catenin signaling pathway regulates E-cadherin expression via the expression of the E-cadherin repressor Snail, the expression of β-catenin after X-irradiation was examined. After 24 hours of irradiation, β-catenin expression increased in non-transfected cells or SUN1_916-depleted cells, whereas β-catenin expression remained unchanged and did not increase in SUN1- or SUN1_888-depleted cells. Therefore, in this study, we found that low-dose X-irradiation induces EMT, and LINC complex component SUN1, especially SUN1_888, is required for X-ray-induced EMT via activation of the Wnt/β-catenin signaling pathway.

Keywords: epithelial-mesenchymal transition (EMT); SUN1; linker of nucleoskeleton and cytoskeleton (LINC) complex; sublethal-dose X-ray

INTRODUCTION

Radiation therapy is commonly used in a wide range of malignant tumors [1–4]. High-precision radiation therapy, comprising intensity modulated radiation therapy and volumetric-modulated arc therapy, has been used in many cancer treatments including prostate cancer, lung cancer and breast cancer [5–7]. However, high-precision radiation therapy delivers low-dose X-ray to the periphery of the target tumor because of multi-directional irradiation [8]. Many studies have shown that low-dose photon irradiation activates cell migration in various cell types, including glioma, pancreatic cancer and breast cancer cells [9–11]. These studies suggest that photon irradiation can increase the metastatic risk, if undetectable tumor cells are scattered around the edges of the irradiated field set for the target volume. Photon-induced aggressive behavior in cancer cells which is a photon-induced metastatic risk, involves various processes such as induction of epithelial-mesenchymal transition (EMT), secretion of matrix

metalloprotease, and upregulation of the expression of integrins [12–15]. However, there is still little way to control photon-induced aggressive behavior.

Mammalian Sad1-UNC-84 proteins (SUNs) are encoded by five genes, SUN1–5. SUN1 and SUN2 are widely expressed in mammalian somatic cells, whereas SUN3, SUN4 (sperm associated antigen4, SPAG4) and SUN5 (SPAG4 Like, SPAG4L) are especially expressed in the germ cells [16–20]. The INM proteins, SUNs and the outer nuclear membrane-spanning (ONM) nuclear envelope spectrin repeat proteins (nesprins) interact with each other in the perinuclear space through luminal domain, SUN and KASH (Klarsicht/Anc-1/Syne1 homology), respectively [17]. SUNs interact with the nucleoskeleton, including chromatin and nuclear lamina [21]. Nesprins interact with the cytoskeleton, including actin filaments, intermediate filaments and microtubule motors [21]. SUNs and nesprins form a multifunctional nuclear membrane protein assembly, and called the linker of nucleoskeleton and cytoskeleton (LINC) complex. The LINC complex affects cellular functions, including nuclear migration, nuclear shaping and positioning, mechanotransduction, DNA repair and cell migration [21–26].

The LINC complex components SUN1 and SUN2 are involved in cell motility, including neuronal migration and cell migration [11, 27]. Furthermore, SUN1 is more important for cell migration and X-ray-enhanced cell migration than SUN2 [11, 28]. The human SUN1 gene has 22 exons and undergoes alternative splicing to generate various splicing variants, including the largest SUN1 splicing variant SUN1_916, which is made up of 916 amino acids (AA) and SUN1_888, which encodes 888 AA. These SUN1 splicing variants play critical roles in the functions of cell migration and X-ray-enhanced cell migration [11, 28]. In addition, a recent study suggested that SUN1 is involved in transforming growth factor-β(TGF-β) induced EMT-associated proteins N-cadherin and vimentin [29].

EMT is an important indicator of malignancy and plays a central role in metastasis. EMT refers to the biological process in which epithelial cells are transformed into mesenchymal cells characterized by loss of adhesion and enhanced migratory ability which is involved in cancer metastasis [30]. EMT is characterized by the downregulation of epithelial molecular markers such as E-cadherin and the upregulation of mesenchymal molecular markers such as N-cadherin, Slug and Snail [31, 32]. Earlier studies revealed that high-dose photon irradiation induces EMT [33, 34], and high-dose radiation-induced EMT is relevant to many signaling pathways, such as the TGF-β pathway, Wnt/β-catenin pathway and phosphoinositide 3 kinase (PI3K)/Akt pathway [35–37]. However, it is unclear whether sublethal-dose, but not high-dose, X-ray induces EMT.

Therefore, in this study, we examined whether sublethal-dose X-irradiation induces EMT and whether the LINC complex component SUN1 is involved in low-dose X-ray-induced EMT.

MATERIALS AND METHODS

Cell culture

The human breast cancer cell line MDA-MB-231 was cultured in Dulbecco's modified Eagle's medium (DMEM) Low glucose (FUJIFILM Wako Pure Chemical Corporation, Osaka, Japan) with 10% fetal bovine serum (FBS; Gibco; Thermo Fisher Scientific, MA, USA) and incubated at 37°C with 10% CO_2 in a humidified incubator.

The human sarcoma cell line HT-1080 used in the supplementary data was grown in Eagle minimum essential medium (EMEM) containing 1% non-essential AA (FUJIFILM Wako Pure Chemical Corporation) and 10% FBS (Gibco; Thermo Fisher Scientific), and maintained in a humidified incubator at 37°C with 5% CO_2.

siRNA transfection

siRNA against the SUN1 cording region (siSUN1, #1,GCACAAACAAAUCAGCUUU; #2,GGUAACUGCUGGGCAUUUA; #3,GAACACAGCGGGUGGAUGA; #4,CGACACAGCUUUCCAAAUA), siRNA against SUN1_916 cording region (siSUN1_916, #1,GGAUGGCCACCUCAGUGUA: #2, UGCCAGUUACUAUGGGAGA), siRNA against SUN1_888 cording region (siSUN1_888, GGCGACGACUGUAAGGGCA) and negative control siRNA (siNC) were transfected into cells using Lipofectamine RNAi MAX (Invitrogen; Thermo Fisher Scientific, MA, USA) and Opti-MEM (Gibco; Thermo Fisher Scientific). In this study, siRNAs #1, #2, #3 and #4 against SUN1 were used for SUN1 knockdown. The siSUN1, siSUN1_916, siSUN1_888 and siNC were obtained from NIPPON GENE Co.

X-irradiation

For X-irradiation, the culture medium was replaced with serum-free medium immediately before X-irradiation as build-up. Cells were irradiated with 4 MV X-ray in a linear accelerator (PRIMUS-KD2; SIEMENS, Munich, Germany) at Kawasaki Medical School Hospital. The dose rate was 2 Gy/min. The medium was replaced with fresh medium containing 10% FBS, immediately after X-irradiation.

Colony formation assay

Immediately after X-irradiation, non-irradiated and irradiated cells were harvested with trypsin–EDTA (FUJIFILM Wako Pure Chemical Corporation), generated single-cell and seeded at 500 cells: non-irradiation, 600 cells: 0.5 Gy, 1000 cells: 2 Gy or 10000 cells: 10 Gy into 6 cm-diameter culture dishes. After incubation for 14 days, the cells were fixed with 4% paraformaldehyde and stained with a 0.04% crystal violet solution. More than 50 cells in each colony were counted as surviving colonies. Surviving fractions (SF) against physical doses (0.5, 2 and 10 Gy) were plotted and fitted to surviving curves using the following linear-quadratic model: $SF = \exp(-\alpha D - \beta D^2)$. D is the X-ray radiation dose.

Cell migration assay

Cell migration was assessed using a 48-microchemotaxis chamber (Neuro Probe, Maryland, USA) and a polycarbonate filter with 8-μm pores (Neuro Probe). The lower side of the filter was precoated with 10 μg/mL collagen type I-C (Nitta Gelatin, Osaka, Japan). A medium containing 10% FBS was placed in the bottom chamber. Non-irradiated and irradiated cells were trypsinized, washed twice with serum-free medium and suspended in serum-free medium supplemented with 0.1% bovine serum albumin (BSA; FUJIFILM Wako Pure Chemical Corporation). Fifty microliters of cell suspension containing 1.1×10^5 MDA-MB-231 cells were added to the upper wells, and incubated for 3 hours. The cells were fixed with 4% paraformaldehyde and stained with hematoxylin. The number of cells that migrated to the lower

side through the pores was counted at ×40 magnification in three independent fields. At least three experiments were conducted.

Matrigel invasion assay

Chemotaxicell filters (Kurabo, Osaka, Japan) with 8-μm pores were precoated with 100 μg/mL Matrigel (Corning, New York, USA). Non-irradiated and irradiated cells were trypsinized, washed twice with serum-free medium and suspended in serum-free medium containing 0.1% BSA. Culture medium with 10% FBS (700 μL) was added to the bottom wells, and 100 μL of the cell suspension containing 5×10^4 MDA-MB-231 cells was added to the upper wells. After incubation at 37°C for 24 hours, cells were fixed with 4% paraformaldehyde and stained with hematoxylin. The number of cells that invaded the lower side through the pores was counted at ×40 magnification in three independent fields. At least three experiments were conducted.

Cell morphology observation

To study changes in cellular morphology, non-transfected cells and siRNA-transfected cells were incubated for 24 hours after irradiation. These cells were observed under a microscope CKX31 (Olympus, Tokyo, Japan) and images (×10 magnification) were obtained.

Western blotting

The cells were lysed in sample buffer (FUJIFILM Wako Pure Chemical Corporation). Cell lysates were sonicated and heated at 95°C for 5 minutes. Samples were separated on 10% polyacrylamide gels (FUJIFILM Wako Pure Chemical Corporation). The proteins were transferred to nitrocellulose membranes, and the membranes were blocked in PBST (PBS solution with 0.05% tween20) containing 3% skim milk or 2% BSA. The membranes were incubated overnight with primary antibodies directed against γH2AX (Cell Signaling Technology [CST], MA, USA), E-cadherin (Invitrogen; Thermo Fisher Scientific), N-cadherin (Invitrogen; Thermo Fisher Scientific), Slug (CST), Snail (CST), β-catenin (Santa Cruz Biotechnology, Texas, USA), β-actin (Sigma-Aldrich, St. Louis, USA) or β-tubulin (CST) at 4°C. Subsequently, the membranes were washed in PBST three times and incubated with secondly antibody (ECL™ anti-rabbit IgG or anti-mouse IgG, horseradish peroxidase linked whole antibody) for 1 hour. Washing of membranes was repeated with PBST three times, and luminescence from horseradish peroxidase was detected using an Amersham™ Imager 680 (Cytiva, Danaher, Washington D.C., USA) using ECL™ Prime Western blotting Detection Reagent (Cytiva). The relative band intensity was quantified using ImageJ [38] and normalized to β-tubulin. At least three experiments were conducted.

Immunofluorescence staining

Cells were washed once with phosphate buffered saline (PBS), fixed in 4% paraformaldehyde solution for 20 minutes and permeabilized with 0.5% Triton X-100 in PBS for 5 minutes at room temperature (RT). The cells were washed with PBS three times and blocked for 30 minutes in 3% BSA in PBS at RT. They were incubated with primary antibodies against SUN1 (Sigma-Aldrich) or β-catenin (Santa Cruz Biotechnology) for 1 hour at RT. The cells were washed with PBS three times, and incubated with fluorescein isothiocyanate (FITC) AffiniPure Donkey Anti-Rabbit IgG (Jackson ImmunoResearch Laboratory, Inc., Suffolk, UK) for 1 hour at RT. The cells were viewed under an epifluorescence microscope IX83 (Olympus).

Polymerase chain reaction

Total RNA was isolated using the PureLink RNA Mini Kit (Invitrogen; Thermo Fisher Scientific) and reverse transcribed using Prime Script RT reagent (Takara, Shiga, Japan). The expression levels of SUN1 variants mRNA and glyceraldehyde-3-phosphatate dehydrogenase (GAPDH) were assessed by reverse transcription polymerase chain reaction (RT-PCR) using the EmeraldAmp PCR Master Mix (Takara). The thermal cycling parameters were 26 cycles or 28 cycles of 98°C for 10 seconds, 55°C for 30 seconds and then 72°C for 1.5 minutes for SUN1_916 or SUN1_888, respectively. The PCR products were analyzed using 6% TBE gel (Invitrogen; Thermo Fisher Scientific) electrophoresis for SUN1 variants and 1% agarose gel electrophoresis for GAPDH. Sequences of the primers used were as follows: SUN1 variants, 5'-GACCACTTCTGGGGTCTTGA-3′ and 5′-GTTTCGAAGGCACCTGGTAA-3′; GAPDH, 5'-GAAGGTGAAG GTCGGAGTC-3′ and 5'-GAAGATGGTGATGGGATTTC-3′.

Statistics

The results are expressed as the mean value with standard deviation. Statistical significance was tested using Student's t-test. Statistical significance was set at $P < 0.01$.

RESULTS

Low-dose X-irradiation induced EMT

We first evaluated clonogenic survival using a colony formation assay to define the sublethal-dose in the human breast cancer cell line MDA-MB-231 cell, which is a triple negative breast cancer cell line. In the colony formation assay, cell survival was dose-dependently decreased by X-irradiation (0.5, 2 and 10 Gy). In this study, an approximately 85% survival dose 0.5 Gy was defined as a sublethal-dose of X-irradiation (Fig. 1A; SF against physical doses (0.5, 2 and 10 Gy) were plotted and fitted to surviving curves using the following linear-quadratic model: $SF = \exp(-\alpha D - \beta D^2)$. $\alpha = 3 \times 10^{-1}$, $\beta = 3 \times 10^{-2}$. D is the X-ray radiation dose.). In addition, we evaluated the expression of γH2AX as DNA damage by Western blotting. The results showed that 0.5 Gy X-irradiation did not increase the expression of γH2AX although 2 Gy X-irradiation increased it (Fig. 1B). Cell migration and invasion activities were examined using the Boyden chamber assay and Matrigel invasion assay after low-dose X-irradiation. Consistent with the results from the past research [11], sublethal-dose 0.5 Gy X-irradiation, but not 2 Gy X-irradiation, enhanced cell migration and invasion (Figs 1C and 1D).

To examine the underlying mechanism of sublethal-dose X-ray-enhanced cell migration and invasion, we focused on photon irradiation-induced EMT [32, 33]. Interestingly, we observed that cell morphology was obviously altered 24 hours after X-irradiation (Fig. 1E). Although non-irradiated cells exhibited an oval shape, cells irradiated with single doses of 0.5 Gy or 2 Gy X-ray displayed elongated spindle-like morphologies, suggesting an EMT-like phenotype (Fig. 1E). We thus, assessed the effects of X-irradiation on the expression of EMT-associated proteins using Western blotting.

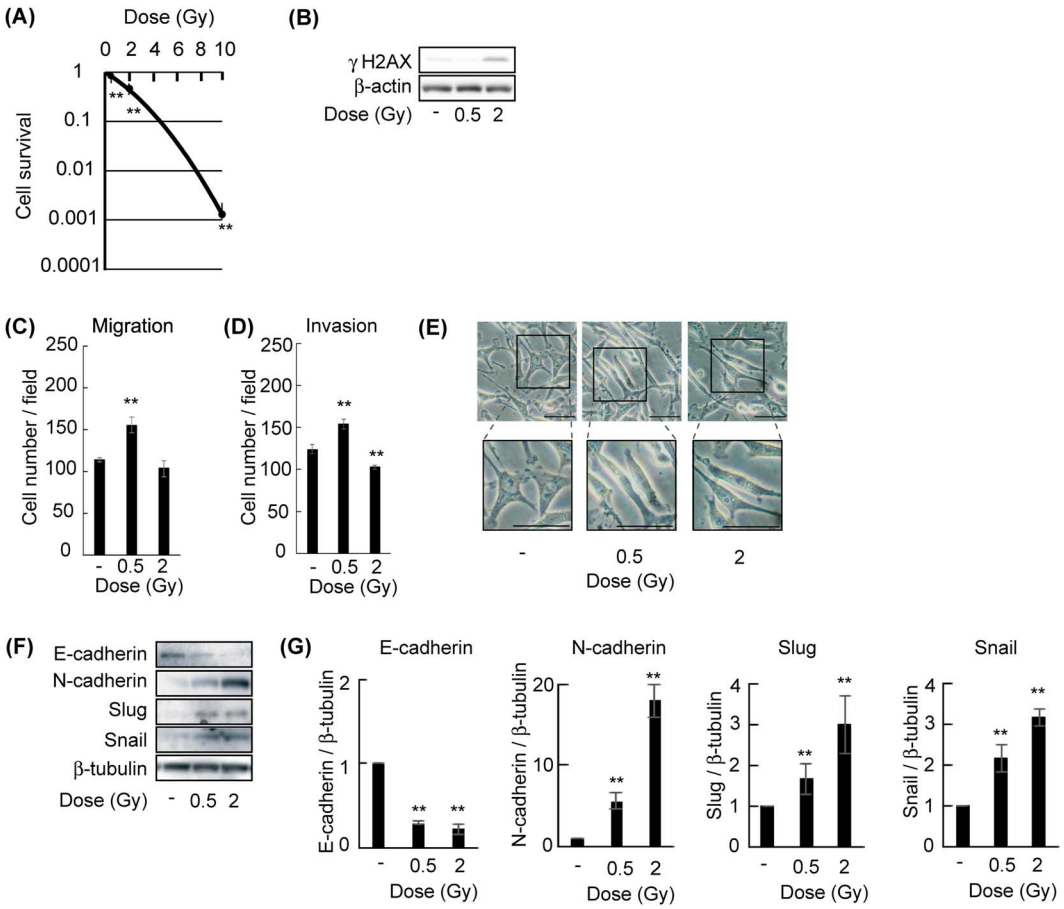

Fig. 1. Sublethal-dose X-irradiation induced changes in cell migration, cell invasion, cell morphology and EMT-associated protein expression. A, Clonogenic survival curves after X-irradiation. MDA-MB-231 cells were exposed to X-ray, and colony formation assays were performed. Each bar represents the mean ± standard deviation. **: $P < 0.01$ vs non-irradiated cells. B, Cells were exposed to the indicated doses of radiation and incubated for 24 hours. The expression of γH2AX was examined using Western blotting. C, Cells were exposed to the indicated doses of X-ray, and migration activities were examined 24 hours later. Each bar represents the mean ± standard deviation. **: $P < 0.01$ vs non-irradiated cells. D, Cells were exposed to the indicated doses of X-ray, and invasion activities were examined 24 hours later. Each bar represents the mean ± standard deviation. **: $P < 0.01$ vs non-irradiated cells. E, Cells were exposed to the indicated doses of X-ray, and morphologies of MDA-MB-231 cells were examined with phase-contrast microscopy. The scale bar represents 50 μm. F and G, Cells were exposed to the indicated doses of X-ray. Twenty-four hours later, the expression of EMT-associated proteins (E-cadherin, N-cadherin, Slug and Snail) was examined by Western blotting. Each bar represents the mean ± standard deviation. **: $P < 0.01$ vs non-irradiated cells.

The results showed that X-irradiation caused a significant reduction in E-cadherin expression and a remarkable increase in the expression of N-cadherin, Slug and Snail (Fig. 1F). The altered expression of EMT-associated proteins, suggestive of EMT was confirmed by quantitative analysis. After 0.5 Gy or 2 Gy X-irradiation, the expression of E-cadherin was reduced to approximately 30% or 20%, whereas the expression of N-cadherin, Slug and Snail was increased approximately 6- or 18-fold, 1.6- or 3-fold and 2- or 3-fold, respectively, compared to that in non-irradiated cells (Fig. 1G). Therefore, these results demonstrate that low-dose, for example, sublethal-dose, X-irradiation induces EMT.

The expression of SUN1 was increased after X-irradiation

We previously showed that the LINC complex component SUN1 plays an important role in cell migration, and that X-irradiation increased the mRNA expression level of SUN1 [11, 28]. Thus, we analyzed the SUN1 by immunofluorescence staining. SUN1 was localized to nuclear envelope, and its expression level was obviously increased by 0.5 Gy or 2 Gy X-irradiation, in MDA-MB-231 cells (Fig. 2A). The upregulated protein expression levels of SUN1 were further evaluated using Western blotting. SUN1 expression was increased by 0.5 Gy or 2 Gy X-irradiation (Figs 2B and 2C). In addition, in HT-1080 cells,

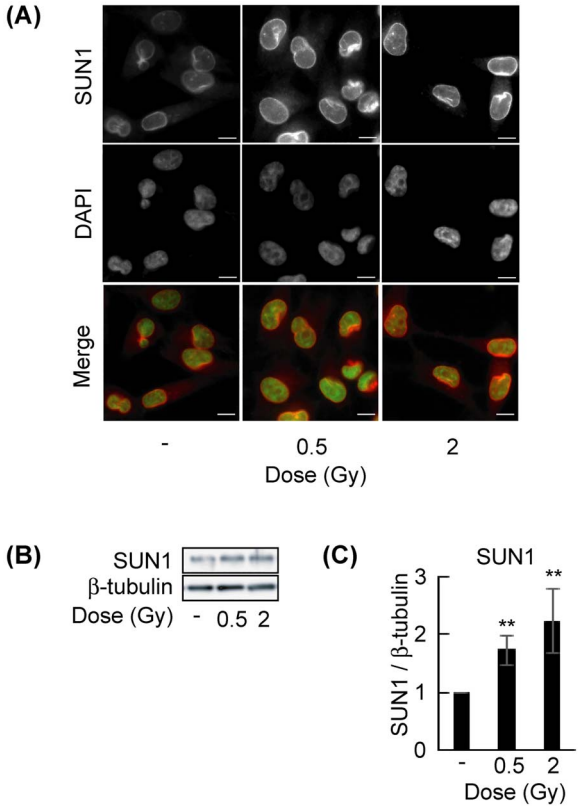

Fig. 2. The expression of SUN1 was increased after X-irradiation in MDA-MB-231 cells. A, MDA-MB-231 cells were exposed to the indicated doses of X-ray. Twenty-four hours after irradiation, the expression of SUN1 was examined by immunofluorescence staining. B and C, Cells were exposed to the indicated doses of radiation and incubated for 24 hours. The expression of SUN1 was assessed by Western blotting. Each bar represents the mean ± standard deviation. **: $P < 0.01$ vs non-irradiated cells.

we confirmed the X-irradiation induced increase in SUN1 expression (Figs S1A, S1B and S1C).

SUN1-depletion suppressed X-ray-induced EMT

Since a recent study suggested that SUN1 is involved in regulating TGF-β-induced EMT-associated protein expression such as N-cadherin and vimentin [29], we investigated whether SUN1 is necessary for X-ray-induced EMT. Therefore, SUN1 was depleted using siRNA. Depletion of SUN1 using siRNA was confirmed by Western blotting (Fig. 3A; siSUN1: #1, #2, #3 and #4). siSUN1-transfected cells were exposed to 0.5 Gy or 2 Gy of X-ray. Twenty-four hours later, changes in the cell morphology were observed. The irradiated negative control siRNA (siNC)-transfected cells exhibited spindle-shaped and elongated morphologies, whereas the irradiated siSUN1-transfected cells did not exhibit elongated spindle-like morphologies (Fig. 3B).

The expression of EMT-associated proteins was analyzed by Western blotting. In the absence of X-irradiation, there were no differences in protein expressions of E-cadherin, N-cadherin, Slug, or Snail between siNC- and siSUN1-transfected cells (Figs 3C, S2A and S2B). In siNC-transfected cells, 0.5 Gy or 2 Gy X-irradiation caused a reduction in E-cadherin expression, in contrast, the expression of N-cadherin, Slug and Snail increased (Figs 3C and 3D). In siSUN1-transfected cells, the expression of E-cadherin, N-cadherin, Slug and Snail proteins did not change after 0.5 Gy or 2 Gy X-irradiation (Figs 3C and 3D). This suggests that SUN1 is required for the X-ray-induced EMT.

SUN1_888, a splicing variant of SUN1 is required for X-ray-induced EMT

The mammalian SUN1 gene generates various splicing variants, including SUN1_888 and SUN1_916 [18, 28]. Since SUN1 splicing variant SUN1_888 but not SUN1_916 is required for X-ray-enhanced cell migration [11], we analyzed the function of SUN1 splicing variants in X-ray-induced EMT. Splicing variant specific siRNAs were transfected into MDA-MB-231 cells to specifically decrease SUN1_916 or SUN1_888. The cells were then exposed to X-ray and incubated for 24 hours. Depletions of SUN1_888 or SUN1_916 using variant-specific siRNA are shown by PCR (Figs 4A and S3A; siSUN1_916: #1 or #2). In the cell morphology after 0.5 Gy or 2 Gy X-irradiation, siSUN1_888-transfected cells exhibited oval shapes compared to siNC-transfected cells. In contrast, siSUN1_916-transfected cells showed elongated spindle-like morphologies indicating EMT-like phenotype (Figs 4B and S3B).

Next, the expression of EMT-associated proteins was assessed using Western blotting. In the absence of X-irradiation, there were no differences in the expression of E-cadherin, N-cadherin, Slug and Snail among siNC-, siSUN1_888- and siSUN1_916-transfected cells (Figs 4C, S4A, S4B, S5A and S5B). siSUN1_916-transfected cells were similar to siNC-transfected cells, decreased E-cadherin expression and dramatically increased the expression of N-cadherin, Slug and Snail, by 0.5 Gy or 2 Gy X-irradiation (Figs 4C, 4D, S5C and S5D). Surprisingly, in siSUN1_888-transfected cells, there were no changes in E-cadherin, N-cadherin, Slug and Snail 24 hours after 0.5 Gy or 2 Gy X-irradiation (Figs 4C and 4D). Therefore, these data demonstrate that SUN1_888 is necessary for low-dose X-ray-induced EMT.

SUN1_888 is required for X-ray-induced β-catenin expression

The Wnt/β-catenin signaling pathway regulates E-cadherin expression level through the expression of E-cadherin repressors, for example, Snail [39, 40]. Thus, we analyzed the expression of β-catenin by Western blotting 24 hours after X-irradiation. The results showed that the expression level of β-catenin protein was increased by 0.5 Gy or 2 Gy X-irradiation in siNC-transfected cells (Fig. 5A). In addition, siSUN1_916-transfected cells showed that β-catenin expression was dramatically increased by low-dose X-irradiation (Figs 5A and S6A). In contrast, siSUN1- or siSUN1_888-transfected cells exhibited that β-catenin protein expression was not amplified by low-dose X-irradiation (Fig. 5A). Quantitative analysis data supported these results (Figs 5B and S6B).

Next, β-catenin expression was evaluated by immunofluorescence staining. The results demonstrated that β-catenin was mainly

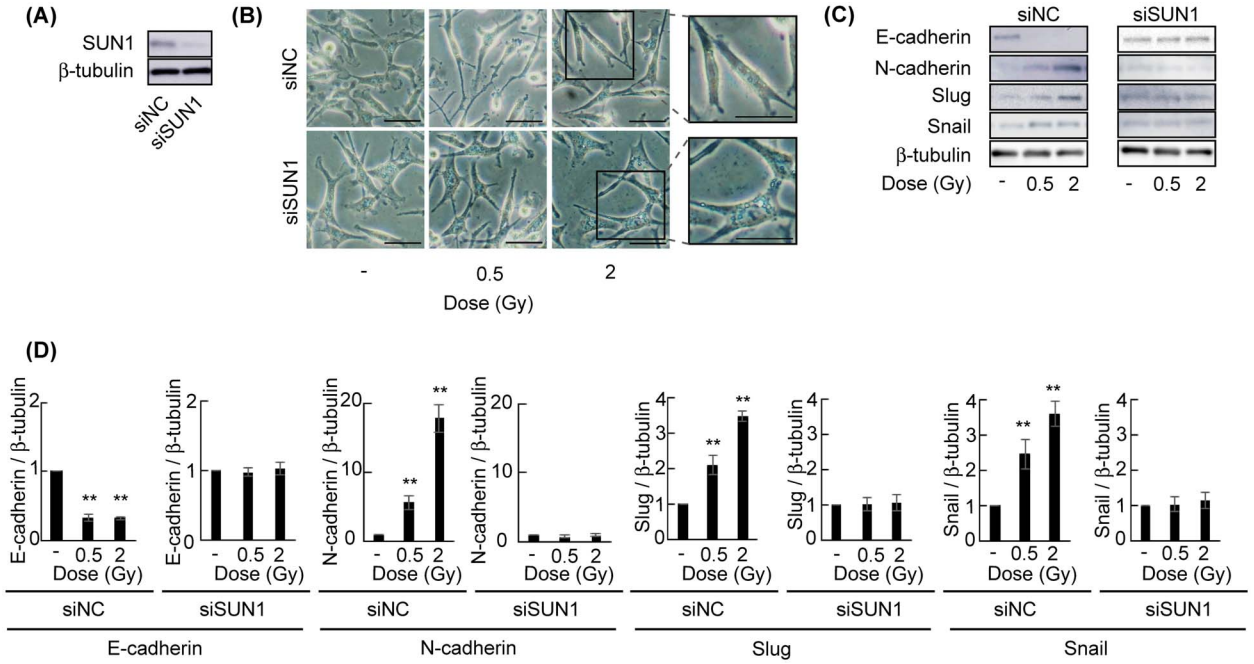

Fig. 3. SUN1 was required for X-ray-induced EMT. A, MDA-MB-231 cells were transfected with siRNA targeting SUN1 (siSUN1) and incubated for 48 hours. The SUN1 expression level was analyzed by Western blotting. B, Cells were transfected with siSUN1 and incubated for 48 hours. These cells were then exposed to X-ray, and after 24 hours of incubation, cell morphologies were examined with phase-contrast microscopy. The scale bar represents 50 μm. C and D, Cells were transfected with siSUN1 and incubated for 48 hours. These cells were then exposed to X-ray, and after 24 hours of incubation, the expression of EMT-associated proteins (E-cadherin, N-cadherin, Slug and Snail) was examined by Western blotting. Each bar represents the mean ± standard deviation. **: $P < 0.01$ vs non-irradiated cells.

distributed on the plasma membrane and in the cytoplasm of siNC-transfected MDA-MB-231 cells in the absence of X-irradiation. After X-irradiation, β-catenin levels were increased by low-dose X-irradiation in siNC-transfected cells (Fig. 5C). On the other hand, in the siSUN1- or siSUN1_888-transfected cells, β-catenin expression was not increased by low-dose X-irradiation (Fig. 5C). β-catenin expression was increased by low-dose X-irradiation in siSUN1_916-transfected cells (Figs 5C and S6C). These results show that SUN1, especially SUN1_888 is important for X-ray-induced β-catenin expression.

DISCUSSION

High-precision radiation therapy delivers low-dose X-ray around the target tumor because of the multi-directional irradiation [8]. In addition, low-dose X-irradiation promotes cell migration and invasion [9–11]. In this study, we showed that low-dose X-irradiation altered cell morphologies, decreased the expression of epithelial molecular marker E-cadherin, and increased the expressions of mesenchymal molecular markers N-cadherin, Slug and Snail. These phenomena demonstrate that low-dose X-irradiation induces EMT, which is implicated in cell invasion [41–43]. However, 2 Gy X-irradiation suppressed cell migration activity and induced EMT. This contradiction is because 2 Gy X-irradiation inhibited the expression of the LINC complex components nesprin-1 and -2, which are related to cell migration [11]. Therefore, it is important to reveal the molecular mechanisms underlying the effects of sublethal-dose X-ray-induced EMT in relation to cell invasion and metastasis.

In MDA-MB-231, the expression of SUN1 protein was increased by low-dose X-irradiation. In addition, SUN1 is required for X-ray-enhanced cell migration [11]. Furthermore, other cell line, HT-1080 also showed that the expression of SUN1 protein was increased by low-dose X-irradiation (Fig. S1), and then SUN1 depletion inhibited X-ray-enhanced cell migration, as well. Based on these results, to clarify the relationship between SUN1 and the low-dose X-ray-induced EMT, the increase in SUN1 expression upon irradiation was suppressed by using siRNA. After X-irradiation SUN1-depleted cells were shown not to induce EMT indicated by the unchanging of cell morphologies and EMT-associated protein expression, E-cadherin, N-cadherin, Slug and Snail. Furthermore, although SUN1_916-depleted cells were exhibited to induce EMT by low-dose X-irradiation, indicated by downregulation of E-cadherin and upregulation of N-cadherin, Slug and Snail, SUN1_888-depleted cells were shown not to induce EMT, as in SUN1-depleted cells. EMT is characterized by cadherin-switch, showing the downregulation of E-cadherin while upregulation the N-cadherin [31]. In addition, E-cadherin is negatively regulated by Slug and Snail [44]. In this study, the expression of Slug and Snail was also not altered by sublethal-dose X-irradiation in SUN1- or SUN1_888-depleted cells. Therefore, as shown in Fig. 5D, the LINC complex component SUN1, or SUN1 splicing variant SUN1_888, is required for X-ray-induced EMT through a cadherin-switch via

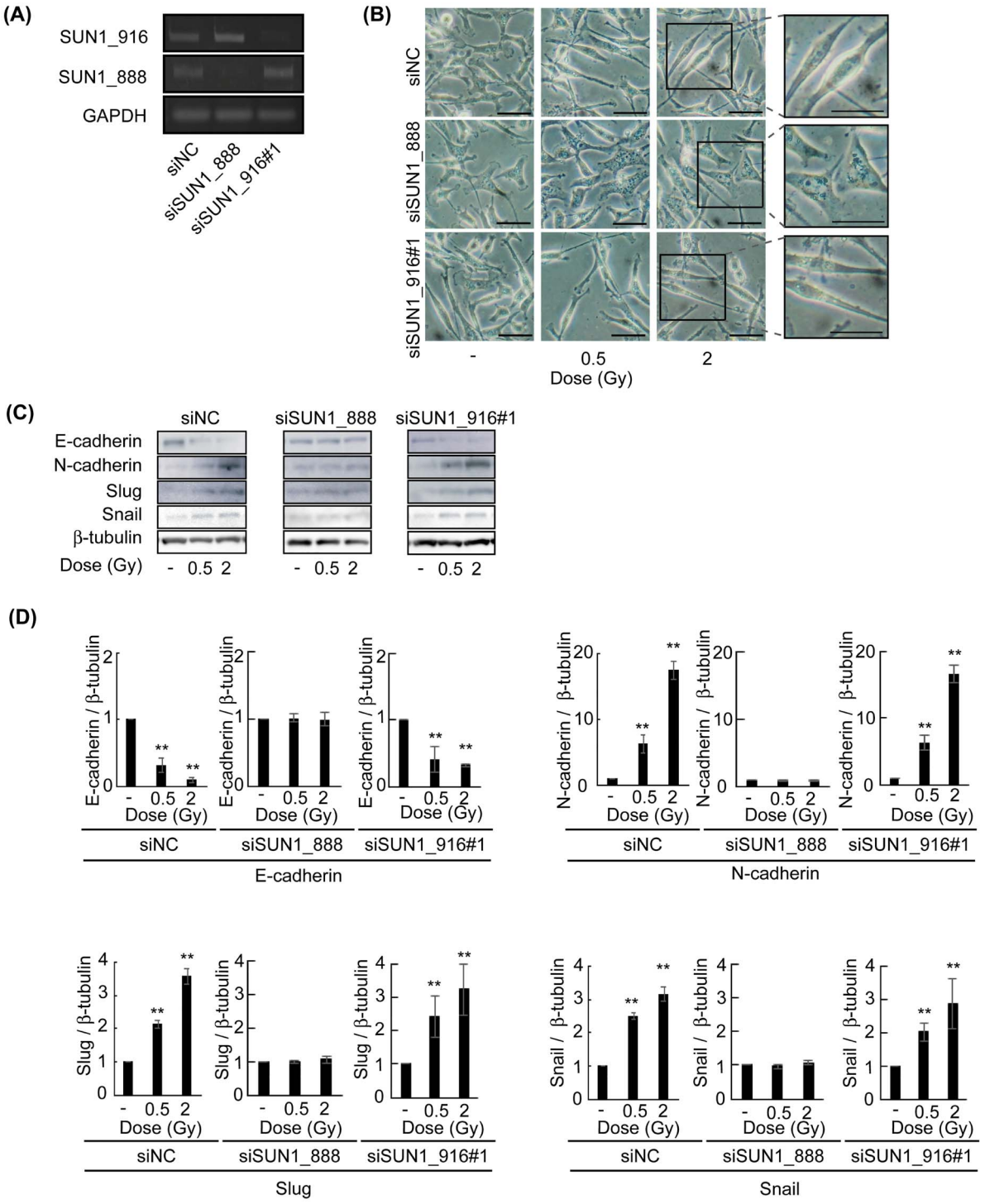

Fig. 4. SUN1 splicing variant SUN1_888 was required for X-ray-induced EMT. A, Each indicated siRNA was transfected into MDA-MB-231 cells for 48 hours. SUN1_916 and SUN1_888 mRNA expression levels were analyzed by PCR. B, Each indicated siRNA was transfected into cells and incubated for 48 hours. These cells were then exposed to X-ray, and after 24 hours of incubation morphologies of cells were examined with phase-contrast microscopy. The scale bar represents 50 μm. C and D, Each indicated siRNA was transfected into cells for 48 hours. These cells were exposed to X-ray, and after 24 hours of incubation, the expression of EMT-associated proteins (E-cadherin, N-cadherin, Slug and Snail) was analyzed by Western blotting. Each bar represents the mean ± standard deviation. **: $P < 0.01$ vs non-irradiated cells.

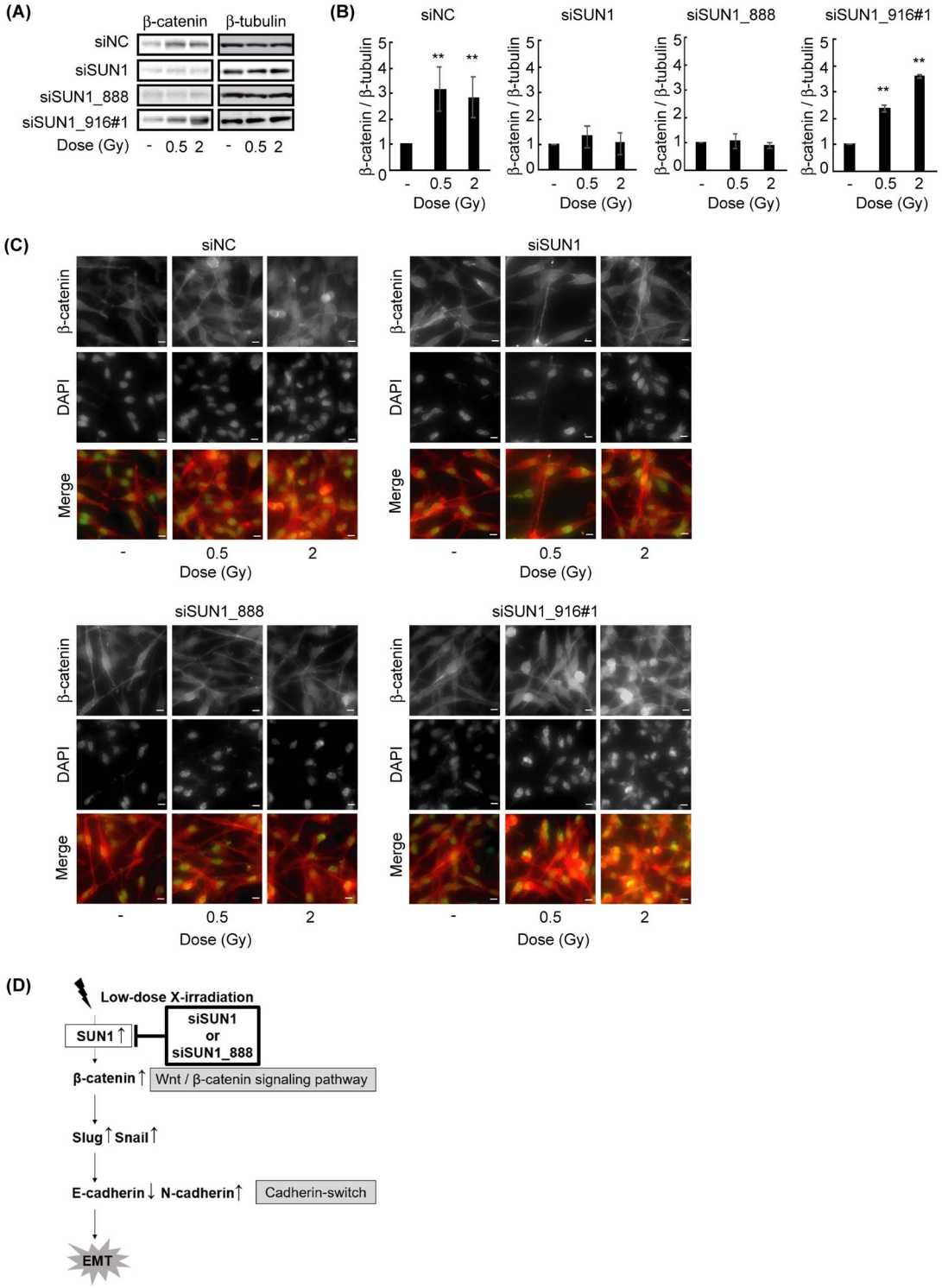

Fig. 5. SUN1 was important for X-ray-induced β-catenin expression. A and B, Each indicated siRNA was transfected into MDA-MB-231 cells for 48 hours. These cells were then exposed to X-ray, and after 24 hours of incubation the expression of β-catenin was examined by Western blotting. Each bar represents the mean ± standard deviation. **: $P < 0.01$ vs non-irradiated cells. C, Each indicated siRNA was transfected into cells for 48 hours. These cells were then exposed to X-ray. The expression and distribution of β-catenin were analyzed by immunofluorescence staining 24 hours later. The scale bar represents 10 μm. D, Schematic illustration showing the relationship between SUN1 and X-ray-induced EMT.

the expression of the E-cadherin repressor Snail. In addition, this study showed that X-irradiation increased β-catenin expression. Furthermore, in SUN1_916-depleted cells, β-catenin expression was increased by X-irradiation. In contrast, the expression of β-catenin did not change in SUN1- or SUN1_888-depleted cells after X-irradiation. These results indicated that X-ray-induced β-catenin expression is required for LINC complex component SUN1, especially SUN1_888. Based on these results, we considered the following mechanisms. The activation of Wnt signaling inhibits β-catenin degradation via inhibition of glycogen synthase kinase (GSK)-3β [45, 46]. Thus, β-catenin is increased by activation of the Wnt/β-catenin signaling pathway, and partly enters the nucleus [46]. β-catenin then binds to transcription factor T-cell factor/lymphoid enhancer factor (TCF/LEF) [47, 48]. The transcription factor TCF/LEF replaces the transcriptional repressor complex Grocho/Histone Deacetylase (HDAC), EMT effectors such as Slug and Snail are activated, and induces EMT [49, 50]. In addition, the PI3K/Akt signaling pathway accumulates β-catenin through inhibition of GSK-3β, and nuclear transport of β-catenin induces EMT [51, 52]. The LINC complex is related to the nuclear transport of β-catenin through nuclear pores [53, 54]. Therefore, nuclear envelope protein SUN1_888 rather than SUN1_916 has critical domain for β-catenin nuclear import or mRNA nuclear export and be related to the Wnt/β-catenin signaling pathway and the PI3K/Akt signaling pathway.

In the TGF-β signaling pathway, Smad2 and Smad3 mediate signaling through cooperation with Smad4 [55, 56]. Smad proteins transmit signals from the cell membrane to nucleus via nuclear transport [55, 57], and this transmission induces EMT [55]. Therefore, the LINC complex might also be necessary for the nuclear transport of Smad. Furthermore, in the Hippo signaling pathway, a recent study reported that Yes-associated protein (YAP) controls the expression of the epithelial marker E-cadherin via the expression of EMT-associated transcription factors Slug and Snail [58]. Additionally, LINC complex component is required for the activation of the YAP signaling pathway through nuclear transport of YAP [59–61]. Therefore, together with the results of this study, the LINC complex component SUN1 may be important for the nuclear transport of YAP and be involved in the Hippo signaling pathway described above. However, many studies in the past have revealed that photon-induced EMT is implicated in various mechanisms, including the activation of the ERK pathway and Rho protein families [62, 63]. Because the LINC complex interacts with both the nucleoskeleton and cytoskeleton, the LINC complex components might be upstream regulators of some of the above molecular mechanisms through mechanotransduction that changes physical forces into chemical reactions via cytoskeleton [64, 65].

This study provided that low-dose X-irradiation induces EMT, and the LINC complex component SUN1 plays an important role in low-dose X-ray-induced EMT, which has not previously been considered. However, to suppress malignancy and metastasis, further studies are needed to reveal various cell signaling pathways via LINC complex components using numerous cultured cells.

SUPPLEMENTARY DATA

Supplementary data are available at *RADRES Journal* online.

ACKNOWLEDGMENTS

We thank Kawasaki Medical School Central Research Institute, staff of the Radiotherapy Department and the Breast and Thyroid Surgery Department at Kawasaki Medical School Hospital. We also thank Dr. Katsunobu Konno and Dr. Seiichi Yamada of Kawasaki University of Medical Welfare for their advice on X-irradiation methods.

CONFLICT OF INTEREST

The authors declare no conflicts of interest associated with this manuscript.

FUNDING

This study was supported by a Grant-in-Aid for Early-Career Scientists from the Japan Society for the Promotion of Science (JSPS) to Hiromasa Imaizumi (grant number 20K16838).

REFERENCES

1. Delaney G, Jacob S, Featherstone C *et al.* The role of radiotherapy in cancer treatment: estimating optimal utilization from a review of evidence-based clinical guidelines. *Cancer* 2005;104:1129–37.
2. Numasaki H, Nakada Y, Okuda Y *et al.* Japanese structure survey of radiation oncology in 2015. *J Radiat Res* 2022;63:230–46.
3. Tyldesley S, Delaney G, Foroudi F *et al.* Estimating the need for radiotherapy for patients with prostate, breast, and lung cancers: verification of model estimates of need with radiotherapy utilization data from British Columbia. *Int J Radiat Oncol Biol Phys* 2011;79:1507–15.
4. Barton MB, Jacob S, Shafiq J *et al.* Estimating the demand for radiotherapy from the evidence: a review of changes from 2003 to 2012. *Radiother Oncol* 2014;112:140–4.
5. Fischer-Valuck BW, Rao YJ, Michalski JM. Intensity-modulated radiotherapy for prostate cancer. *Transl Androl Urol* 2018;7:297–307.
6. Chan C, Lang S, Rowbottom C *et al.* Intensity-modulated radiotherapy for lung cancer: current status and future developments. *J Thorac Oncol* 2014;9:1598–608.
7. Karpf D, Sakka M, Metzger M *et al.* Left breast irradiation with tangential intensity modulated radiotherapy (t-IMRT) versus tangential volumetric modulated arc therapy (t-VMAT): trade-offs between secondary cancer induction risk and optimal target coverage. *Radiat Oncol* 2019;14:156.
8. Krueger EA, Fraass BA, McShan DL *et al.* Potential gains for irradiation of chest wall and regional nodes with intensity modulated radiotherapy. *Int J Radiat Oncol Biol Phys* 2003;56:1023–37.
9. Wild-Bode C, Weller M, Rimner A *et al.* Sublethal irradiation promotes migration and invasiveness of glioma cells: implications for radiotherapy of human glioblastoma. *Cancer Res* 2001;61:2744–50.
10. Qian LW, Mizumoto K, Urashima T *et al.* Radiation-induced increase in invasive potential of human pancreatic cancer cells and its blockade by a matrix metalloproteinase inhibitor, GCS27023. *Clin Cancer Res* 2002;8:1223–7.

11. Imaizumi H, Sato K, Nishihara A *et al.* X-ray-enhanced cancer cell migration requires the linker of nucleoskeleton and cytoskeleton complex. *Cancer Sci* 2018;109:1158–65.
12. Fujita M, Otsuka Y, Yamada S *et al.* X-ray irradiation and rho-kinase inhibitor additively induce invasiveness of the cells of the pancreatic cancer line, MIAPaCa-2, which exhibits mesenchymal and amoeboid motility. *Cancer Sci* 2011;102:792–8.
13. Cheng JCH, Chou CH, Kuo ML *et al.* Radiation-enhanced hepatocellular carcinoma cell invasion with MMP-9 expression through PI3K/Akt/NF-kappaB signal transduction pathway. *Oncogene* 2006;25:7009–18.
14. Jung JW, Hwang SY, Hwang JS *et al.* Ionising radiation induces changes associated with epithelial-mesenchymal transdifferentiation and increased cell motility of A549 lung epithelial cells. *Eur J Cancer* 2007;43:1214–24.
15. Ogata T, Teshima T, Kagawa K *et al.* Particle irradiation suppresses metastatic potential of cancer cells. *Cancer Res* 2005;65:113–20.
16. Hodzic DM, Yeater DB, Bengtsson L *et al.* SUN2 is a novel mammalian inner nuclear membrane protein. *J Biol Chem* 2004;279:25805–12.
17. Crisp M, Liu Q, Roux K *et al.* Coupling of the nucleus and cytoplasm: role of the LINC complex. *J Cell Biol* 2006;172:41–53.
18. Göb E, Schmitt J, Benavente R *et al.* Mammalian sperm head formation involves different polarization of two novel LINC complexes. *PLoS One* 2010;5:e12072.
19. Shao X, Tarnasky HA, Lee JP *et al.* Spag4, a novel sperm protein, binds outer dense-fiber protein Odf1 and localizes to microtubules of manchette and axoneme. *Dev Biol* 1999;211:109–23.
20. Frohnert C, Schweizer S, Hoyer-Fender S. SPAG4L/SPAG4L-2 are testis-specific SUN domain proteins restricted to the apical nuclear envelope of round spermatids facing the acrosome. *Mol Hum Reprod* 2011;17:207–18.
21. Bone CR, Starr DA. Nuclear migration events throughout development. *J Cell Sci* 2016;129:1951–61.
22. Gundersen GG, Worman HJ. Nuclear positioning. *Cell* 2013;152:1376–89.
23. Wilhelmsen K, Ketema M, Truong H *et al.* KASH-domain proteins in nuclear migration, anchorage and other processes. *J Cell Sci* 2006;119:5021–9.
24. Chambliss AB, Khatau SB, Erdenberger N *et al.* The LINC-anchored actin cap connects the extracellular milieu to the nucleus for ultrafast mechanotransduction. *Sci Rep* 2013;3:1087.
25. Lei K, Zhu X, Xu R *et al.* Inner nuclear envelope proteins SUN1 and SUN2 play a prominent role in the DNA damage response. *Curr Biol* 2012;22:1609–15.
26. Chancellor TJ, Lee J, Thodeti CK *et al.* Actomyosin tension exerted on the nucleus through nesprin-1 connections influences endothelial cell adhesion, migration, and cyclic strain-induced reorientation. *Biophys J* 2010;99:115–23.
27. Zhang X, Lei K, Yuan X *et al.* SUN1/2 and Syne/Nesprin-1/2 complexes connect centrosome to the nucleus during neurogenesis and neuronal migration in mice. *Neuron* 2009;64:173–87.
28. Nishioka Y, Imaizumi H, Imada J *et al.* SUN1 splice variants, SUN1_888, SUN1_785, and predominant SUN1_916, variably function in directional cell migration. *Nucleus* 2016;7:572–84.
29. Chi YH, Wang WP, Hung MC *et al.* Deformation of the nucleus by TGFβ1 via the remodeling of nuclear envelope and histone isoforms. *Epigenetics Chromatin* 2022;15:1.
30. Moreno-Bueno G, Portillo F, Cano A. Transcriptional regulation of cell polarity in EMT and cancer. *Oncogene* 2008;27:6958–69.
31. Rosso M, Majem B, Devis L *et al.* E-cadherin: a determinant molecule associated with ovarian cancer progression, dissemination and aggressiveness. *PLoS One* 2017;12:e0184439.
32. Mikami S, Katsube K, Oya M *et al.* Expression of snail and slug in renal cell carcinoma: E-cadherin repressor snail is associated with cancer invasion and prognosis. *Lab Investig* 2011;91:1443–58.
33. Kim RK, Kaushik N, Suh Y *et al.* Radiation driven epithelial-mesenchymal transition is mediated by notch signaling in breast cancer. *Oncotarget* 2016;7:53430–42.
34. Zhang H, Luo H, Jiang Z *et al.* Fractionated irradiation-induced EMT-like phenotype conferred radioresistance in esophageal squamous cell carcinoma. *J Radiat Res* 2016;57:370–80.
35. Wang J, Kang M, Wen Q *et al.* Berberine sensitizes nasopharyngeal carcinoma cells to radiation through inhibition of Sp1 and EMT. *Oncol Rep* 2017;37:2425–32.
36. Bastos LG, de Marcondes PG, De-Freitas-Junior JC *et al.* Progeny from irradiated colorectal cancer cells acquire an EMT-like phenotype and activate Wnt/β-catenin pathway. *J Cell Biochem* 2014;115:2175–87.
37. Lee YJ, Han HJ. Troglitazone ameliorates high glucose-induced EMT and dysfunction of SGLTs through PI3K/Akt, GSK-3β, Snail1, and β-catenin in renal proximal tubule cells. *Am J Physiol Renal Physiol* 2010;298:F1263–75.
38. Schneider CA, Rasband WS, Eliceiri KW. NIH image to ImageJ: 25 years of image analysis. *Nat Methods* 2012;9:671–5.
39. Wu ZQ, Li XY, Hu CY *et al.* Canonical Wnt signaling regulates slug activity and links epithelial-mesenchymal transition with epigenetic breast cancer 1, early onset (BRCA1) repression. *Proc Natl Acad Sci U S A* 2012;109:16654–9.
40. Moon JH, Lee SH, Lim YC. Wnt/β-catenin/slug pathway contributes to tumor invasion and lymph node metastasis in head and neck squamous cell carcinoma. *Clin Exp Metastasis* 2021;38:163–74.
41. Kang Y, Massagué J. Epithelial-mesenchymal transitions: twist in development and metastasis. *Cell* 2004;118:277–9.
42. Neelakantan D, Zhou H, Oliphant MUJ *et al.* EMT cells increase breast cancer metastasis via paracrine GLI activation in neighbouring tumour cells. *Nat Commun* 2017;8:15773.
43. He E, Pan F, Li G *et al.* Fractionated ionizing radiation promotes epithelial-mesenchymal transition in human esophageal cancer cells through PTEN deficiency-mediated Akt activation. *PLoS One* 2015;10:e0126149.
44. Peinado H, Portillo F, Cano A. Transcriptional regulation of cadherins during development and carcinogenesis. *Int J Dev Biol* 2004;48:365–75.
45. Megason SG, McMahon AP. A mitogen gradient of dorsal midline Wnts organizes growth in the CNS. *Development* 2002;129:2087–98.
46. Huang J, Guo X, Li W *et al.* Activation of Wnt/β-catenin signalling via GSK3 inhibitors direct differentiation of human adipose stem cells into functional hepatocytes. *Sci Rep* 2017;7:40716.

47. Behrens J, von Kries JP, Kühl M *et al.* Functional interaction of beta-catenin with the transcription factor LEF-1. *Nature* 1996;382:638–42.
48. van de Wetering M, Cavallo R, Dooijes D *et al.* Armadillo coactivates transcription driven by the product of the drosophila segment polarity gene dTCF. *Cell* 1997;88:789–99.
49. Daniels DL, Weis WI. Beta-catenin directly displaces Groucho/TLE repressors from Tcf/Lef in Wnt-mediated transcription activation. *Nat Struct Mol Biol* 2005;12:364–71.
50. Medici D, Hay ED, Olsen BR. Snail and slug promote epithelial-mesenchymal transition through beta-catenin-T-cell factor-4-dependent expression of transforming growth factor-beta3. *Mol Biol Cell* 2008;19:4875–87.
51. Lee S, Choi EJ, Cho EJ *et al.* Inhibition of PI3K/Akt signaling suppresses epithelial-to-mesenchymal transition in hepatocellular carcinoma through the snail/GSK-3/beta-catenin pathway. *Clin Mol Hepatol* 2020;26:529–39.
52. Wu K, Fan J, Zhang L *et al.* PI3K/Akt to GSK3β/β-catenin signaling cascade coordinates cell colonization for bladder cancer bone metastasis through regulating ZEB1 transcription. *Cell Signal* 2012;24:2273–82.
53. Uzer G, Bas G, Sen B *et al.* Sun-mediated mechanical LINC between nucleus and cytoskeleton regulates βcatenin nuclear access. *J Biomech* 2018;74:32–40.
54. Déjardin T, Carollo PS, Sipieter F *et al.* Nesprins are mechanotransducers that discriminate epithelial-mesenchymal transition programs. *J Cell Biol* 2020;219:e201908036.
55. Valcourt U, Kowanetz M, Niimi H *et al.* TGF-beta and the Smad signaling pathway support transcriptomic reprogramming during epithelial-mesenchymal cell transition. *Mol Biol Cell* 2005;16:1987–2002.
56. Chang H, Brown CW, Matzuk MM. Genetic analysis of the mammalian transforming growth factor-beta superfamily. *Endocr Rev* 2002;23:787–823.
57. Shi Y, Massagué J. Mechanisms of TGF-beta signaling from cell membrane to the nucleus. *Cell* 2003;113:685–700.
58. Cheng D, Jin L, Chen Y *et al.* YAP promotes epithelial mesenchymal transition by upregulating slug expression in human colorectal cancer cells. *Int J Clin Exp Pathol* 2020;13:701–10.
59. Driscoll TP, Cosgrove BD, Heo S-J *et al.* Cytoskeletal to nuclear strain transfer regulates YAP signaling in mesenchymal stem cells. *Biophys J* 2015;108:2783–93.
60. Owens DJ, Fischer M, Jabre S *et al.* Lamin mutations cause increased YAP nuclear entry in muscle stem cells. *Cell* 2020;9:816.
61. Aureille J, Buffière-Ribot V, Harvey BE *et al.* Nuclear envelope deformation controls cell cycle progression in response to mechanical force. *EMBO Rep* 2019;20:e48084.
62. Nagarajan D, Melo T, Deng Z *et al.* ERK/GSK3β/snail signaling mediates radiation-induced alveolar epithelial-to-mesenchymal transition. *Free Radic Biol Med* 2012;52:983–92.
63. Tan S, Yi P, Wang H *et al.* RAC1 involves in the radioresistance by mediating epithelial-mesenchymal transition in lung cancer. *Front Oncol* 2020;10:649.
64. Uzer G, Rubin CT, Rubin J. Cell mechanosensitivity is enabled by the LINC nuclear complex. *Curr Mol Biol Rep* 2016;2:36–47.
65. Yi X, Wright LE, Pagnotti GM *et al.* Mechanical suppression of breast cancer cell invasion and paracrine signaling to osteoclasts requires nucleo-cytoskeletal connectivity. *Bone Res* 2020;8:40.